BIOCHEMISTRY
including biophysical chemistry & molecular biology

Article

pubs.acs.org/biochemistry

Conduction and Block of Inward Rectifier K^+ Channels: Predicted Structure of a Potent Blocker of Kir2.1

Tamsyn A. Hilder* and Shin-Ho Chung

Computational Biophysics Group, Research School of Biology, Australian National University, Canberra, ACT 0200, Australia

ABSTRACT: Dysfunction of Kir2.1, thought to be the major component of inward currents, I_{K1}, in the heart, has been linked to various channelopathies, such as short Q-T syndrome. Unfortunately, currently no known blockers of Kir2.*x* channels exist. In contrast, Kir1.1b, predominantly expressed in the kidney, is potently blocked by an oxidation-resistant mutant of the honey bee toxin tertiapin (tertiapin-Q). Using various computational tools, we show that both channels are closed by a hydrophobic gating mechanism and inward rectification occurs in the absence of divalent cations and polyamines. We then demonstrate that tertiapin-Q binds to the external vestibule of Kir1.1b and Kir2.1 with K_d values of 11.6 nM and 131 μM, respectively. We find that a single mutation of tertiapin-Q increases the binding affinity for Kir2.1 by 5 orders of magnitude (K_d = 0.7 nM). This potent blocker of Kir2.1 may serve as a structural template from which potent compounds for the treatment of various diseases mediated by this channel subfamily, such as cardiac arrhythmia, can be developed.

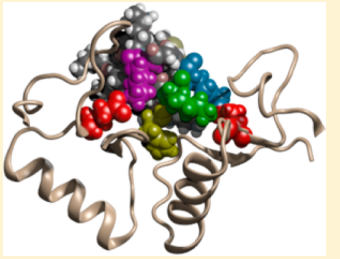

Inwardly rectifying potassium (Kir) channels selectively allow potassium ions to move more freely into, rather than out of, the cell.[1] They maintain the membrane resting potential and regulate the action potential in electrically excitable cells.[1] There are seven subfamilies of the Kir family (from Kir1.*x* to Kir7.*x*), each family composed of one to four members, and these are classified into four functional groups, including (i) classical Kir channels (Kir2.*x*), (ii) G protein-gated Kir channels (Kir3.*x*), (iii) ATP-sensitive Kir channels (Kir6.*x*), and (iv) K^+ transport channels (Kir1.*x*, Kir4.*x*, Kir5.*x*, and Kir7.*x*). An opportunity to clarify the physical basis of inward rectification and gating of two Kir channels arises: the weakly rectifying Kir1.1b isoform (ROMK2 or ROMK1B) and the strongly rectifying Kir2.1 (IRK1). Kir1.1b is a constitutively active, ATP-regulated Kir channel[1] expressed in the kidney[2,3] and various brain tissues.[4] Kir2.1 is thought to be the major component of I_{K1} current in heart,[1] which is essential for the stable resting potential and long plateau that is a feature of the cardiac action potential.[4] Both channels have been linked to various channelopathies. For example, loss-of-function mutations in Kir1.1 cause Bartter's syndrome[1,5] and in Kir2.1 cause type 1 Andersen syndrome and catecholaminergic polymorphic ventricular tachycardia.[1,6] Gain-of-function mutations in Kir2.1 cause familial atrial fibrillation and short Q-T syndrome.[1,6] Moreover, evidence that loss of function in glial Kir channels plays an important role in epileptogenesis is accumulating, and Kir2.1 channels have been identified in a type of glial cell in the hippocampus.[7] Therefore, Kir2.1 channels may provide a new target for the treatment of various neurological and cardiac diseases, such as epilepsy and ventricular fibrillation.

There are three outstanding issues to be resolved. First, the precise physical basis for inward rectification of all Kir channels remains to be elucidated. A generally held view is that outward currents are totally or partially blocked by intracellular cations, such as Mg^{2+} and polyamines.[1,3,7−10] Inward rectification is observed in the absence of these cations when charged residues in the cytoplasmic domain of Kir1.1b and Kir2.1 are mutated to alanine.[6,11−13] The binding of one or more of these divalent ions to the cytoplasmic domain of the channel is believed to occlude the ion-conducting conduit, either physically or electrostatically.[8,9,11−13] Some Kir channels, however, exhibit inward rectification in the absence of intracellular divalent ions (such as in endothelial cells),[14] although the degree of rectification becomes more pronounced in their presence.[4,14−17] Unlike in KcsA, neutral, hydrophobic residues guard the intracellular gate of all Kir channels. When the phenylalanine residue at position 192 is replaced with an acidic residue in Kir3.2, the current−voltage relationship of the F192E mutant channel, determined computationally, becomes linear, thus suggesting that the lack of acidic residues at the intracellular gate causes outward currents to be attenuated.[18]

Second, the structural changes involved in Kir channel gating are largely unknown. The movement of TM2 pore helices away from the permeation pathway is believed to underlie the opening of inward rectifiers.[1,5,19] It has also been noted that the cytoplasmic segment of some inward rectifiers is normally devoid of water molecules. Conduction events take place when the entire conduit is filled with water molecules.[18,20] These two events, namely, the movement of TM2 pore helices and hydration of the pore, may be related, one preceding the other. Generally, the cytoplasmic gate of inward rectifiers is lined with hydrophobic amino acid residues, such as leucine in Kir1.1,[1] methionine in Kir2.1,[21] and phenylalanine in Kir3.2.[18] The inner segment of the pore may become hydrated following a translational or rotational motion of these hydrophobic residues.

Received: November 4, 2012
Revised: January 7, 2013

dx.doi.org/10.1021/bi301498x | *Biochemistry* XXXX, XXX, XXX−XXX

Finally, a blocker of inward rectifiers, tertiapin-Q (TPN_Q), is potent for some Kir channels, while ineffective on other channels. TPN_Q is an oxidation-resistant mutant of the 21-residue polypeptide toxin tertiapin isolated from the honey bee. For example, the polypeptide toxin blocks Kir1.1 with a K_d value of 1.3 nM[22] but is relatively insensitive to Kir2.1 with a K_d value of 20 μM.[23] Despite being 45% identical in sequence, these two channels have markedly different affinities for TPN_Q. There are currently no known specific blockers of Kir2.*x* channels.[1] It will be of interest to modify the toxin to become an effective blocker of the Kir2.1 channel. A compound that can reduce or block I_{K1} may act as a potent inhibitor of re-entry-type arrhythmias and ventricular fibrillation[24] and provide a novel means of enhancing cardiac contractility.[23,25] An effective inhibitor of Kir2.1, if it can be designed, can be used as a structural template for developing new therapeutic agents.

In the computational studies reported here, we address these three issues. Using several state-of-the-art computational tools, we examine the K^+ conduction mechanism, the cause of inward rectification, and the binding of TPN_Q to two Kir channels, Kir1.1b and Kir2.1. First, we generate homology models of the Kir1.1b and Kir2.1 channels and compare their conductance characteristics to experimentally determined values. We demonstrate that inward rectification occurs in the absence of intracellular blockers such as Mg^{2+}, and that the channels are controlled by a hydrophobic gating mechanism. We then compare the binding of TPN_Q to the Kir1.1b and Kir2.1 channels to aid in the development of a more potent blocker of Kir2.1. Using these models, we determine the potential of mean force encountered by TPN_Q as it approaches the extracellular entrance to both the Kir1.1b and Kir2.1 channels. Finally, we determine the potential of mean force for our mutated toxin and demonstrate its ability to potently block Kir2.1. Our findings led to a better understanding of the mechanisms underlying the permeation of K^+ ions across the inward rectifiers and to the development of a targeted pharmaceutical.

THEORETICAL CALCULATIONS

Homology Modeling. Amino acid sequences of the Kir1.1b and Kir2.1 ion channels are obtained from the National Center for Biotechnology Information (NCBI) protein database (NCBI entries NP_722449.2 and NP_000882.1, respectively). The sequences are analyzed using BLAST[26] revealing (a) 71% sequence identity between Kir2.1 and Kir2.2 [3JYC_A whose crystal structure has been determined to 3.1 Å resolution,[27] Protein Data Bank (PDB) entry 3JYC] and (b) 49% sequence identity between Kir1.1b and the Kir2.2 R186A mutant (3SPG_A whose crystal structure has been determined to 2.6 Å resolution,[28] PDB entry 3SPG). Kir1.1b and Kir2.1 sequences are separately submitted to the modeling server SwissModel (http://swissmodel.expasy.org/) using Automated Mode.[29] Structural models of Kir1.1b and Kir2.1 are generated using the crystal structure coordinates of Kir2.2 (3JYC) and Kir2.2(R186A) (3SPG) as templates. Model quality is evaluated using the standard tools available in SwissModel, and no further changes are required. Tetramers with 4-fold symmetry are created from each of the monomer models, using the transformation matrices from the PDB coordinate files. The new structural models are refined using MD simulations in a vacuum.

Brownian Dynamics Simulations. Brownian dynamics (BD) simulations are used to determine the conductance of ions through Kir1.1b and Kir2.1 channels. This allows us to evaluate our models against experiment by comparing our calculated conductance to those determined experimentally. We run five simulations, each lasting 10 million time steps (1 μs) with a symmetrical KCl concentration of 140 mM. The current is calculated using the relationship $I = qn/\Delta t$, where n is the average number of ions that cross the membrane, q is the charge of the ion, and Δt is the simulation time of one run. Because the current−voltage curve is pronouncedly nonlinear, the conductance is measured at certain voltages. Both homology models are found to be in the closed configuration because no potassium current is observed in BD simulations despite there being an unobstructed pathway through the pore. For each Kir channel, the intracellular gate is progressively expanded using highly constrained minimization in molecular dynamics (MD) simulations until the potassium current is observed in BD simulations. A similar method has been used to open the Kir3.2 channel.[18] We find that it is necessary to increase the radius of the entrance to the intracellular gate from 1.0 to 2.4 Å for Kir1.1b and from 1.0 to 3.2 Å for Kir2.1. Detailed descriptions of BD simulations are given by Hoyles et al.[30] and in our previous paper.[18]

Molecular Docking. We use the rigid docking program[31] ZDOCK 3.0.1 to predict the state of TPN_Q bound to both Kir1.1b and Kir2.1. The coordinates of tertiapin are obtained from the PDB (entry 1TER).[32] We then mutate the methionine residue at position 13 of TPN to glutamine, shown in Figure 1,

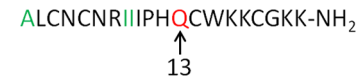

Figure 1. Sequence of TPN_Q with residues 13 (red) and 1, 8, and 9 (green) highlighted.

to create the TPN_Q structure. This structure is used in subsequent simulations. The 600 top-ranked structures are considered as possible docking modes. We search the docked structures for candidates in which one of the six charged residues of TPN_Q (four lysines, one arginine, and one histidine) is docked into the selectivity filter. The histidine at position 12 is shown to occlude the entrance to the pore in six and two of the top-ranked structures for Kir1.1b and Kir2.1, respectively. No other charged residues are observed to dock into the selectivity filter. Because the flexibility of the toxin and protein is not taken into account in ZDOCK, we perform molecular dynamics (MD) simulations to determine the predicted bound state. The highest-ranked docked structure is used as the starting configuration in MD simulations.

Molecular Dynamics Simulations. Molecular dynamics (MD) simulations are used to determine the bound configuration of TPN_Q and the mutated TPN_Q and to calculate their respective profiles of potential of mean force (PMF). All MD simulations are performed using NAMD 2.8 and visualized using VMD 1.9.1.[33,34] All simulations use the CHARMM36 force field[35,36] and TIP3P water with a time step of 2 fs, at constant pressure (1 atm) and temperature (310 K). The Kir−toxin complexes are embedded in a 3-palmitoyl-2-oleoyl-D-glycero-1-phosphatidylcholine (POPC) lipid bilayer, solvated in a 100 Å × 100 Å × 104 Å box of water. Potassium and chloride ions are added both to neutralize the system and to simulate an ionic concentration of 200 mM. The protein is initially held fixed, allowing the water and ions to equilibrate. For the remaining simulations, the protein and lipid bilayer centers of

dx.doi.org/10.1021/bi301498x | *Biochemistry* XXXX, XXX, XXX−XXX

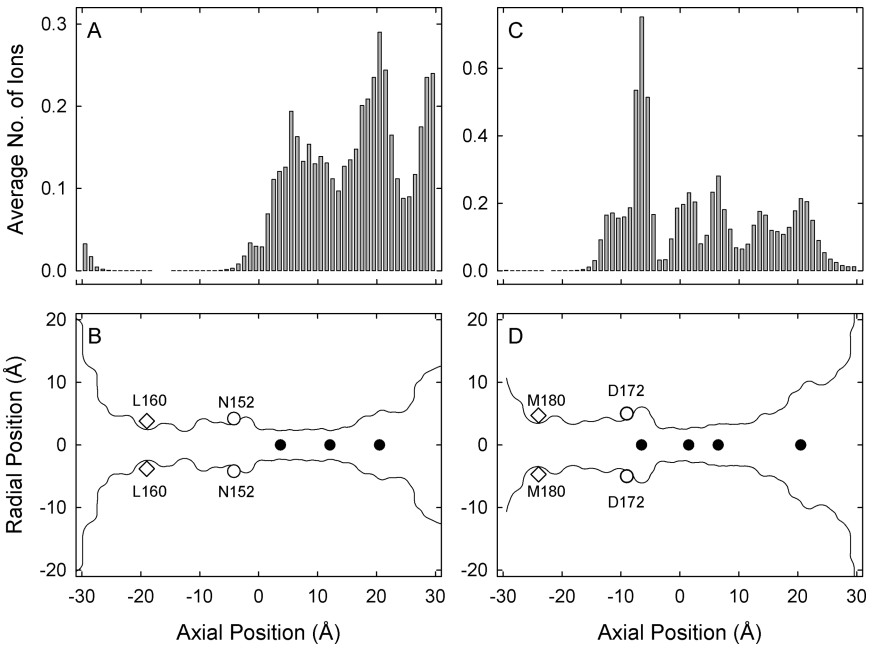

Figure 2. Dwell histogram and the pore outline of Kir1.1b and Kir2.1. To obtain the dwell histograms of Kir1.1b (A) and Kir2.1 (C), the channels are divided into 100 thin sections and the number of ions present in each section over a simulation period of 1 μs is tabulated. Pore outlines in the open state of Kir1.1b (B) and Kir2.1 (D). Filled circles indicate the positions of potassium ions in each channel; empty diamonds are used to indicate the position of the hydrophobic gate residues, and empty circles are used to indicate the position of the aspartate residue at position 172 (D172) and asparagine residue at position 152 (N152). The axial positions at −30 and 30 Å correspond to the intracellular and extracellular sides of the membrane, respectively. The center of mass of the channel is located at 0 Å.

mass are held by a harmonic constraint of 0.2 kcal mol^{-1} Å^{-2}. The entire system is equilibrated for a period of 3−4 ns.

Umbrella sampling is used to determine the PMF for the binding of TPN_Q to Kir1.1b and Kir2.1 and that for the binding of the mutated TPN_Q to Kir2.1. The equilibrated structure is used to generate sampling windows by performing steered molecular dynamics (SMD). A force constant of 30 kcal mol^{-1} Å^{-2} is applied to pull the toxin out of the binding site. During SMD, the protein backbone atoms are held fixed and the root-mean-square-deviation of the backbone atoms of the toxin are maintained by applying a harmonic constraint of 0.2 kcal mol^{-1} Å^{-2}. The channel central axis is used as the reaction coordinate. We construct umbrella sampling windows every 0.5 Å using the continuous configurations generated by SMD. The centers of mass of the backbone atoms of the toxin are constrained to be within an 8 Å cylinder centered on the channel axis, and beyond this, a harmonic potential of 20 kcal mol^{-1} Å^{-2} is applied. This has been shown to provide adequate sampling. In addition, a harmonic potential of 30 kcal mol^{-1} Å^{-2} is applied in the z direction to constrain the center of mass to the sampling window. Each window is run for 5 ns. The PMF is constructed using the weighted histogram analysis method.[37] A similar methodology was used in our previous paper.[18]

Using the PMF, we can determine the binding affinity of the toxin. Specifically, the dissociation constant (K_d) in units of molar is estimated to be[38−40]

$$K_d^{-1} = 1000 N_A \pi R^2 \int_{z_1}^{z_2} \exp[-W(z)/k_B T]\, dz \quad (1)$$

where $W(z)$ is the one-dimensional PMF with the zero point located at bulk, $1000N_A$ is used to convert from cubic meters to liters per mole, k_B and T are Boltzmann's constant and the temperature, respectively, z_1 is in the binding pocket, and z_2 is in the bulk.[40] The windows at 44.0 and 47 Å are assumed to be bulk for Kir2.1 and Kir1.1b, respectively, and therefore, the PMF is set to zero at this point. Equation 1 was originally derived for the binding of an ion to the channel[38] but has since been successfully applied to toxin binding. A hydrogen bond is assumed to be formed if the donor−acceptor distance is <3.0 Å and the donor−hydrogen−acceptor angle is ≥150°. Similarly, a salt bridge is formed if the distance between a basic residue on the toxin and an acidic residue on the channel is <4 Å.

RESULTS AND DISCUSSION

Hydrophobic Gating and Ion Conduction. Both Kir1.1b and Kir2.1 consist of three distinct zones. The selectivity filter, located close to the extracellular side of the membrane, is connected to a water cavity that is 8−10 Å in diameter, which then narrows toward the intracellular side of the membrane forming an intracellular gate. The region from the intracellular gate to the water cavity is surrounded by hydrophobic residues in both Kir1.1b and Kir2.1. In MD simulations of the closed Kir1.1b and Kir2.1 channels, water molecules are not present in this region, but once the intracellular gate is expanded, water floods into the pore. Our results suggest a hydrophobic gating mechanism, also reported for the Kv1.2,[41] acetylcholine receptor,[42] and various Kir[18,20] channels.

Via expansion of the intracellular gate of both Kir1.1b and Kir2.1, the channels are transformed into the open configuration and potassium current is observed. In both channels, a K^+ ion entering from the extracellular vestibule encounters a large energy well. As a result, there are on average 2 and 2.3 ions in the selectivity filter of Kir1.1b and Kir2.1, respectively, in the absence of an externally imposed electric field. There are also, on average, 2.5 and 1.8 ions present in the extracellular vestibule of Kir1.1b and Kir2.1, respectively. No ions reside in the intracellular hydrophobic gate region. A significant difference between the Kir1.1b and Kir2.1 channels is the

dx.doi.org/10.1021/bi301498x | Biochemistry XXXX, XXX, XXX−XXX

additional presence of three ions in the water cavity of Kir2.1. This is most likely due to the presence of an aspartate residue at position 172 of Kir2.1 located at approximately −10 Å. In earlier studies, this aspartate residue has been linked to both intrinsic gating and blockage by Mg^{2+}.[16] Other studies have shown that the water cavity attracts cations only in strong rectifiers.[11] For Kir1.1b, prominent peaks in the dwell histogram (Figure 2A) are located at approximately 3.7 Å (near the T122 carbonyl oxygen), 12.1 Å (near the Y125 carbonyl oxygen), and 20.5 Å (in the extracellular vestibule), as illustrated in Figure 2B. For Kir2.1, ions preferentially dwell (Figure 2C) at z = −6.5 Å (inside the water cavity), 1.5 Å (between the T142 and I143 carbonyl oxygens), and 6.5 Å (near the G144 carbonyl oxygen), as illustrated in Figure 2D.

By examining the two-ion PMFs of these two channels, we are able to obtain a more detailed understanding of the conduction mechanism. Two ions exist in a stable equilibrium within the selectivity filter. When a third ion enters from the extracellular vestibule under the influence of an applied potential, the innermost ion is expelled because of Coulombic repulsion.

Inwardly Rectifying Current−Voltage Relationships. Using BD simulations, we examine the conductance properties of both the Kir1.1b and Kir2.1 channels under various conditions. The current−voltage profiles for Kir1.1b and Kir2.1 wild-type open channels and mutant channels are shown in Figure 3A constructed with a symmetrical concentration of 140 mM KCl. Both wild-type open channels exhibit inward rectification in the absence of divalent cations. For Kir1.1b, we obtain currents of 0 ± 0 and −2.7 ± 0.2 pA at 100 and −100 mV, respectively. The conductance increases from 27 pS at −100 mV to 56 pS at −125 mV. This compares well with experimentally determined values. For instance, Ho et al.[43] obtained a unitary slope conductance of 39 pS in symmetrical 145 mM KCl for Kir1.1, and Zhou et al.[44] obtained a conductance of 30 pS for Kir1.1b in the presence of 110 mM K^+. Although Kir1.1b has an NH_2-terminal amino acid sequence different from that of Kir1.1, it produces identical macroscopic currents and biophysical properties.[2,5]

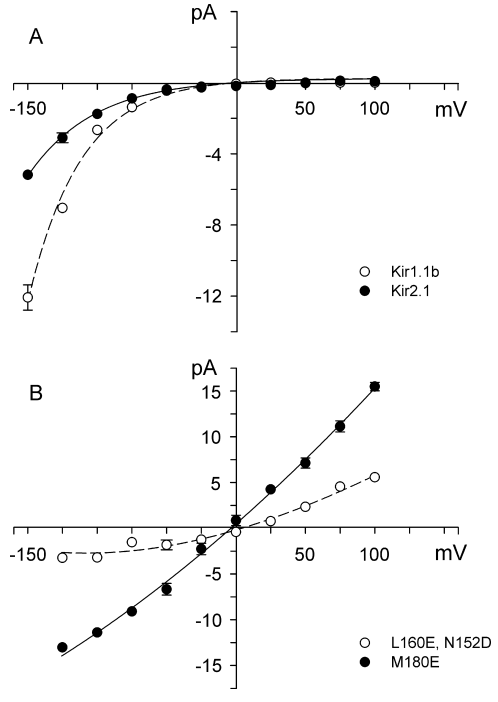

Figure 3. Current−voltage profiles for the Kir1.1b and Kir2.1 channels. (A) Open wild-type Kir1.1b and Kir2.1 channels and (B) L160E, N152D, and M180E mutants of Kir1.1b and Kir2.1 channels. Each data point represents the average of five sets of simulations, each simulation lasting 10 million time steps (1 μs). Error bars represent one standard error of the mean, and error bars smaller than the data points are not shown.

For Kir2.1, we obtain currents of 0.1 ± 0.1 and −1.8 ± 0.1 pA at 100 and −100 mV, respectively. The conductance increases from 18 pS at −100 mV to 25 pS at −125 mV. Again, this compares well with experimentally determined values. For instance, in cell-attached patches, Kubo et al.[45] obtained a conductance of 21 pS with a 140 mM external solution and 90 mM intracellular solution, D'Avanzo et al.[24] obtained a conductance of approximately 19 pS at −100 mV with 140 mM K^+, and Aleksandrov et al.[15] obtained a conductance of 21 pS in 140 mM symmetrical K^+.

We observe inward rectification in the absence of divalent cations in both the Kir2.1 and Kir1.1b channels (see Figure 3A). Aleksandrov et al.[15] found that Kir2.1 displays inward rectification in the absence of divalent ions but inward rectification is enhanced by their presence. One possible reason for the attenuation of outward current may be the lack of acidic residues guarding the intracellular gate. In our previous work,[18] mutating the bulky phenylalanine residue in Kir3.2 removed inward rectification. The leucine residue at position 160 is thought to be the intracellular gate for the Kir1.1b channel.[1,46] Therefore, we mutate this residue to glutamic acid (L160E). The L160E mutant Kir1.1b channel continues to be inwardly rectifying with a current−voltage curve identical to that of the wild-type channel. Sackin et al.[46] found that replacing L160 with smaller glycines abolished pH gating. The current through the channel increases to −5.2 ± 0.6 pA at −100 mV because of the presence of these acidic residues, but still no outward current is observed at 100 mV. In contrast to Kir1.1b, via mutation of the methionine residue at position 180, the Kir2.1 channel is no longer inwardly rectifying. The potassium current becomes 15.5 ± 0.5 and −11.4 ± 0.3 pA at 100 and −100 mV, respectively (Figure 3B). Thus, the effect of replacing a hydrophobic residue near the intracellular gate with a polar residue is different in these two channels. As mentioned, Kir2.1 has an aspartate residue located near the water cavity at position 172. Via mutation of the equivalent residue, an asparagine at position 152, in Kir1.1b to aspartate, the channel is no longer inwardly rectifying (Figure 3B). The potassium current becomes 5.3 ± 0.6 and −3.4 ± 0.6 pA at 100 and −100 mV, respectively.

Binding of Tertiapin-Q. Figure 4 illustrates the PMF for the cleavage of TPN_Q from the Kir2.1 and Kir1.1b channels. The PMF reaches a minimum at 24.0 Å for Kir1.1b, with a well depth of −20.5 kT. For Kir2.1, the PMF reaches a minimum at 20.0 Å with a well depth of −10.6 kT. We find that the binding between TPN_Q and the Kir channels is stable, and therefore, all 5 ns of umbrella sampling is used. It is assumed that the properties for the window at 44.0 and 47.0 Å for Kir2.1 and Kir1.1b, respectively, are similar to those of the bulk, and therefore, the PMF is set to zero at this point.

Using eq 1, we obtain dissociation constants, K_d, of 131 μM and 11.6 nM for Kir2.1 and Kir1.1b channels, respectively. These values are compare well with experimentally determined

dx.doi.org/10.1021/bi301498x | Biochemistry XXXX, XXX, XXX−XXX

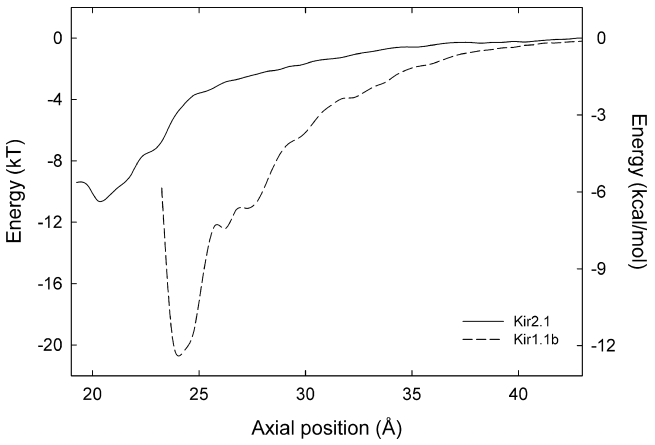

Figure 4. Potential of mean force (PMF) for the cleavage of TPN_Q from the Kir2.1 and Kir1.1b channels. The axial position represents the distance in the *z*-direction from the center of mass of the channel.

values. TPN_Q binds to Kir1.1 with a high affinity (K_d = 1.3 nM),[22] whereas Kir2.1 is insensitive to TPN_Q (K_d = 20 μM).[23]

To characterize the interactions between TPN_Q and the Kir channels, we analyze their hydrogen bonding and salt bridge formation for the umbrella sampling window located at the minimum of the PMF, 20.0 and 24.0 Å for Kir2.1 and Kir1.1b, respectively. In both channels, the H12 residue occludes the entrance to the pore.

Figure 5A demonstrates the stability over the 5 ns simulation of the salt bridges formed between Kir1.1b and TPN_Q. There are three stable salt bridges that form between Kir1.1b and TPN_Q; these K20−E104, K16−E104, and K17−E104 salt bridges are illustrated in Figure 6. Jin et al.[47] studied TPN_Q and Kir1.1. They found that much higher concentrations of TPN_Q are required to inhibit half the Kir1.1 current when residues H12, K17, and K20 are mutated to alanine. Their half-blocking concentrations were 20-, 5-, and 15-fold higher for alanine substitutions at residues H12, K17, and K20, respectively. These same residues are the among the main residue pairs for the binding of TPN_Q to Kir1.1b from our MD simulations. Moreover, Ramu et al.[48] found that TPN_Q inhibition of Kir1.1 is profoundly affected by extracellular pH because of the titration of H12, implying that the positive charge on H12 is critical for high-affinity binding of TPN_Q to Kir1.1. Sensitivity to pH is largely eliminated by mutating the H12 to lysine, and its affinity for the channel increases from 1.3 to 0.18 nM.[48] We investigate the effect of an H12K mutation of the Kir2.1 channel and find that the depth of the PMF increases from −10.6 to −19.1 kT. The affinity of the H12K mutant for the Kir2.1 channel increases from 131 μM to 34.1 nM.

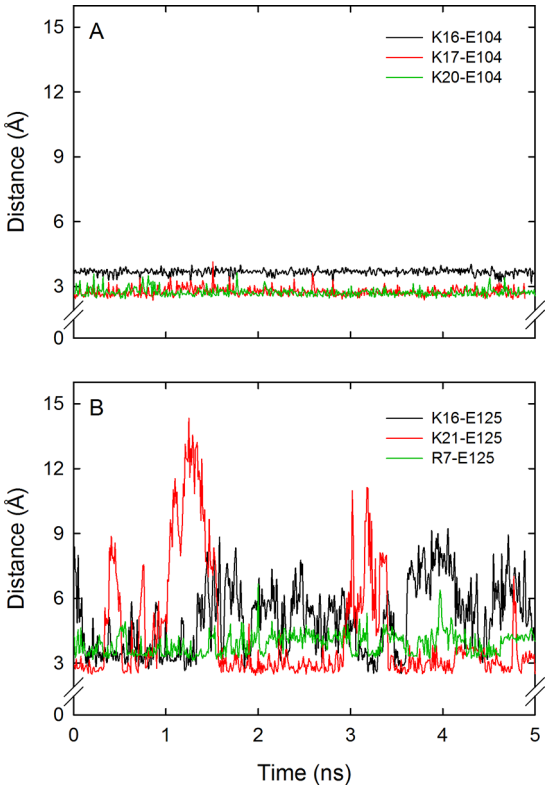

Figure 5. Salt bridge distances for Kir1.1b (A) and Kir2.1 (B) and TPN_Q.

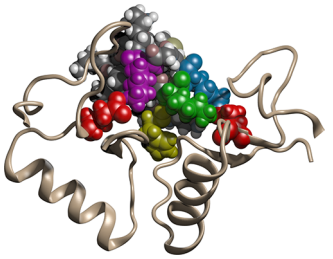

Figure 6. Binding of tertiapin-Q to the outer vestibule of Kir1.1b. Residue H12 (yellow) points into the selectivity filter. Lysine residues K16 (green), K17 (blue), and K20 (pink) are bound to E104 residues of the channel (red). For the sake of clarity, only part of the channel is shown.

In contrast, the salt bridges between Kir2.1 and TPN_Q are relatively unstable compared to those of Kir1.1b (Figure 5B). The salt bridges between K16 and E125 and between K21 and E125 are shown to form and break numerous times throughout the 5 ns simulation. Figure 7 illustrates the Kir2.1−TPN_Q complex. Although both Kir2.1 and Kir1.1b form, on average, three salt bridges with TPN_Q over the entire simulation, only one of these is stable for Kir2.1, whereas all three are stable for Kir1.1b (Figure 5). As a result, TPN_Q binds more strongly to Kir1.1b.

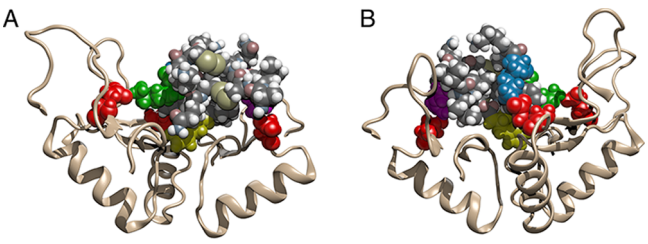

Figure 7. Two views of the binding of tertiapin-Q to the outer vestibule of Kir2.1: (A) front view and (B) back view. Residue H12 (yellow) points into the selectivity filter. Lysine residues K16 (green) and K21 (blue) and arginine residue R7 (pink) are bound to E125 residues of the channel (red). For the sake of clarity, only part of the channel is shown.

Tertiapin-Q Mutation. It would be beneficial to develop a potent blocker of Kir2.1 as this may provide a new target for the treatment of various cardiac diseases, such as ventricular

dx.doi.org/10.1021/bi301498x | *Biochemistry* XXXX, XXX, XXX−XXX

fibrillation. In addition, it would allow detailed investigation of the physiological role of Kir2.1. Initially, we investigate mutations of TPN_Q at three positions, the isoleucine residues at positions 8 and 9 and the alanine residue at position 1, highlighted in Figure 1. The isoleucine residues are mutated to both lysine and arginine, and the alanine residue is mutated to lysine. Umbrella sampling simulations are extremely computationally expensive; therefore, equilibrium MD simulations were run for 2 ns on all five mutations to get a sense of their stability. These simulations demonstrate that mutating the isoleucine residue at position 8 to lysine (I8K) and arginine (I8R) was the most stable change, and therefore, these were run for a further 2 ns. Mutation I8R demonstrated the most stable salt bridges over the 4 ns simulation. In addition, generally more salt bridges exist for the I8R mutation. We will refer to this I8R mutant of TPN_Q as TPN_{RQ}.

To determine the predicted binding of TPN_{RQ}, we determine the PMF for the cleavage from Kir2.1. Figure 8 illustrates the

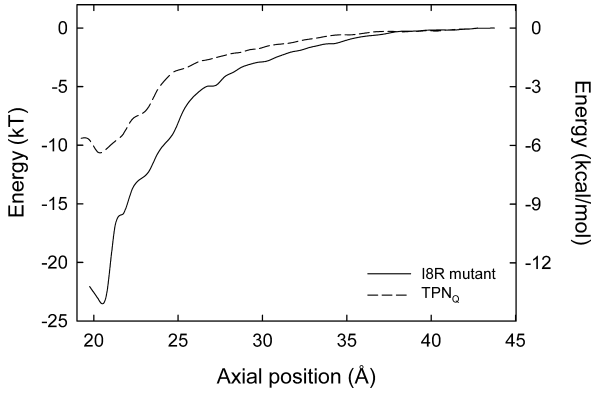

Figure 8. Binding of the I8R mutant of TPN_Q to Kir2.1. PMF of TPN_{RQ} with the original PMF of TPN_Q shown for comparison. The axial position represents the distance in the z-direction from the center of mass of the channel.

PMF for TPN_{RQ}. As shown, the PMF now reaches a minimum at 20.5 Å with the well deepening from −10.6 to −23 kT. Using eq 1, the dissociation constant for TPN_{RQ} is 0.7 nM, which is approximately 10^5 times more potent than TPN_Q.

The I8R mutation increases the stability of the salt bridges formed with Kir2.1. Initially, the lysine residue at position 21 (K21) is bound to the glutamate residue at position 125 (E125) on chain D of Kir2.1. At approximately 1.25 ns, this salt bridge is broken and does not re-form. K21 then forms a salt bridge with E125 on chain A. The main residue pairs are now K21 and E125, R7 and E125, and R8 and E153, which are illustrated in Figure 9.

There are two main reasons for improvement in the binding affinity of TPN_{RQ} for Kir2.1. First, the average number of salt bridges increases so that Kir2.1 now forms, on average, 4.6 salt bridges with TPN_{RQ}. Second, there are now two stable salt bridges, because of the addition of R8 and E153.

CONCLUSIONS

Using BD, we investigate the permeation of an ion through two inward rectifier potassium channels, Kir1.1b and Kir2.1. Our simulated conductances of 27 pS for Kir1.1b and 18 pS for Kir2.1 at −100 mV compare well with experimentally determined values.[15,44] Both models exhibit inward rectification in the absence of divalent cations, similar to that observed by

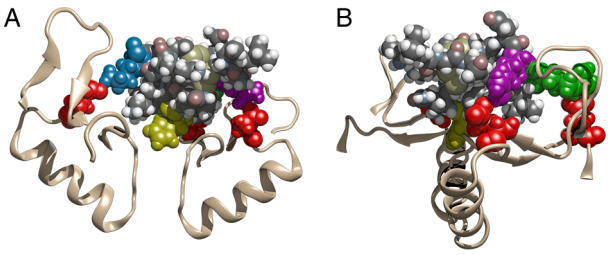

Figure 9. Two views of the binding of TPN_{RQ} to the outer vestibule of Kir2.1: (A) front view and (B) side view. Residue H12 (yellow) points into the selectivity filter. Lysine residue K21 (green) and arginine residues R7 (pink) and R8 (blue) are bound to residues E125 and E153 (red). For the sake of clarity, only part of the channel is shown.

Aleksandrov et al.[15] for Kir2.1. Moreover, our simulations demonstrate that a hydrophobic gating mechanism exists in both Kir2.1 and Kir1.1, similar to that observed by Haider et al.[20]

Using MD simulations, we investigate the binding of TPN_Q to both Kir1.1b and Kir2.1. TPN_Q binds with K_d values of 131 μM and 11.6 nM for Kir2.1 and Kir1.1b channels, respectively, which compare well with experimentally determined values.[22,23] In both channels, His12 occludes the selectivity filter. Unfortunately, there are currently no known blockers of Kir2.1. To compare the binding modes of these two channels, we mutate the isoleucine residue at position 8 of TPN_Q to an arginine residue and predict that it binds to Kir2.1 with a significantly improved K_d value of 0.7 nM. This potent blocker of Kir2.1 may make accessible a new target for the treatment of various cardiac diseases, such as ventricular fibrillation and short Q-T syndrome. Moreover, it could lead to a more detailed understanding of the physiological roles of Kir2.1.

AUTHOR INFORMATION

Corresponding Author

*E-mail: tamsyn.hilder@anu.edu.au. Phone: +61 2 6125 4034. Fax: +61 2 6125 0739.

Author Contributions

The manuscript was written through contributions of all authors. All authors have given approval to the final version of the manuscript.

Funding

We gratefully acknowledge the support from the Australian Research Council through a Discovery Early Career Researcher Award and the National Health and Medical Council.

Notes

The authors declare no competing financial interest.

ACKNOWLEDGMENTS

We thank Dr. Anna Robinson for her scientific advice. Rhys Hawkins from the Visualization Laboratory at the Australian National University and Silvie Ngo provided excellent technical assistance, for which we are grateful. This work was supported by the NCI National Facility at the Australian National University.

ABBREVIATIONS

Kir, inwardly rectifying potassium channel; TPN_Q, tertiapin-Q; MD, molecular dynamics; BD, Brownian dynamics; PMF, potential of mean force; SMD, steered molecular dynamics.

REFERENCES

(1) Hibino, H., Inanobe, A., Furutani, K., Murakami, S., Findlay, I., and Kurachi, Y. (2010) Inwardly rectifying potassium channels: Their structure, function and physiological roles. *Physiol. Rev. 90*, 291−366.

(2) Doupnik, C. A., Davidson, N., and Lester, H. A. (1995) The inward rectifier potassium channel family. *Curr. Opin. Neurobiol. 5*, 268−277.

(3) Reimann, F., and Ashcroft, F. M. (1999) Inwardly rectifying potassium channels. *Curr. Opin. Cell Biol. 11*, 503−508.

(4) Nichols, C. G., and Lopatin, A. N. (1997) Inward rectifier potassium channels. *Annu. Rev. Physiol. 59*, 171−191.

(5) Welling, P. A., and Ho, K. (2009) A comprehensive guide to the ROMK potassium channel: Form and function in health and disease. *Am. J. Physiol. 297*, F849−F863.

(6) Anumonwo, J. M. B., and Lopatin, A. N. (2010) Cardiac strong inward rectifier potassium channels. *J. Mol. Cell. Cardiol. 48*, 45−54.

(7) Neusch, C., Weishaupt, J. H., and Bähr, M. (2003) Kir channels in the CNS: Emerging new roles and implications for neurological diseases. *Cell Tissue Res. 311*, 131−138.

(8) Yang, J., Jan, Y. N., and Jan, L. Y. (1995) Control of rectification and permeation by residues in two distinct domains in an inward rectifier K^+ channel. *Neuron 14*, 1047−1054.

(9) Xie, L. H., John, S. A., Ribalet, B., and Weiss, J. N. (2004) Regulation of gating by negative charges in the cytoplasmic pore in the Kir2.1 channel. *J. Physiol. 561*, 159−168.

(10) Matsuda, H., Saigusa, A., and Irisawa, H. (1987) Ohmic conductance through the inwardly rectifying K^+ channel and blocking by internal Mg^{2+}. *Nature 325*, 156−159.

(11) Robertson, J. L., Palmer, L. G., and Roux, B. (2008) Long-pore electrostatics in inward rectifier potassium channels. *J. Gen. Physiol. 132*, 613−632.

(12) Robertson, J. L., Palmer, L. G., and Roux, B. (2012) Multi-ion distributions in the cytoplasmic domain of inward rectifier potassium channels. *Biophys. J. 103*, 434−443.

(13) Yeh, S. H., Chang, H. K., and Shieh, R. C. (2005) Electrostatics in the cytoplasmic pore produce intrinsic inward rectification in Kir2.1 channels. *J. Gen. Physiol. 126*, 551−562.

(14) Silver, M. R., and DeCoursey, T. E. (1990) Intrinsic gating of inward rectifier in bovine pulmonary artery endothelial cells in the presence or absence of internal Mg^{2+}. *J. Gen. Physiol. 96*, 109−133.

(15) Aleksandrov, A., Velimirovic, B., and Clapham, D. E. (1996) Inward rectification of the IRK1 K^+ channel reconstituted in lipid bilayers. *Biophys. J. 70*, 2680−2687.

(16) Stanfield, P. R., Davies, N. W., Shelton, P. A., Sutcliffe, M. J., Khan, I. A., Brammer, W. J., and Conley, E. C. (1994) A single aspartate residue is involved in both intrinsic gating and blockage by Mg^{2+} of the inward rectifier, IRK1. *J. Physiol. 478*, 1−6.

(17) Lopatin, A. N., and Nichols, C. G. (1996) $[K^+]$ dependence of open-channel conductance in cloned inward rectifier potassium channels (IRK1, Kir2.1). *Biophys. J. 71*, 682−694.

(18) Hilder, T. A., and Chung, S. H. (2013) Conductance properties of the inwardly rectifying channel, Kir3.2: Molecular and Brownian dynamics study. *Biochim. Biophys. Acta 1828*, 471−478.

(19) Kuo, A., Gulbis, J. M., Antcliff, J. F., Rahman, T., Lowe, E. D., Zimmer, J., Cuthbertson, J., Ashcroft, F. M., Ezaki, T., and Doyle, D. A. (2003) Crystal structure of the potassium channel KirBac1.1 in the closed state. *Science 300*, 1922−1926.

(20) Haider, S., Khalid, S., Tucker, S. J., Ashcroft, F. M., and Sansom, M. S. P. (2007) Molecular dynamics simulations of inwardly rectifying (Kir) potassium channels: A comparative study. *Biochemistry 46*, 3643−3652.

(21) Tai, K., Stansfeld, P. J., and Sansom, M. S. P. (2009) Ion-blocking sites of the Kir2.1 channel revealed by multiscale modelling. *Biochemistry 48*, 8758−8763.

(22) Jin, W., and Lu, Z. (1999) Synthesis of a stable form of tertiapin: A high-affinity inhibitor for inward-rectifier K^+ channels. *Biochemistry 38*, 14286−14293.

(23) Ramu, Y., Klem, A. M., and Lu, Z. (2004) Short variable sequence acquired in evolution enables selective inhibition of various inward-rectifier K^+ channels. *Biochemistry 43*, 10701−10709.

(24) D'Avanzo, N., Cho, H. C., Tolokh, I., Pekhletski, R., Tolokh, I., Gray, C., Goldman, S., and Backx, P. H. (2005) Conduction through the inward rectifier potassium channel, Kir2.1, is increased by negatively charged extracellular residues. *J. Gen. Physiol. 125*, 493−503.

(25) Nichols, C. G., Makhina, E. N., Pearson, W. L., Sha, Q., and Lopatin, A. N. (1996) Inward rectification and implications for cardiac excitability. *Circ. Res. 78*, 1−7.

(26) Altschul, S. F., Madden, T. L., Schäffer, A. A., Zhang, J., Zhang, Z., Miller, W., and Lipman, D. J. (1997) Gapped BLAST and PSI-BLAST: A new generation of protein database search programs. *Nucleic Acids Res. 25*, 3389−3402.

(27) Tao, X., Avalos, J. L., Chen, J., and Mackinnon, R. (2009) Crystal structure of the eukaryotic strong inward-rectifier K^+ channel Kir2.2 at 3.1 Å resolution. *Science 326*, 1668−1674.

(28) Hansen, S. B., Tao, X., and MacKinnon, R. (2011) Structural basis of PIP2 activation of the classical inward rectifier K^+ channel Kir2.2. *Nature 477*, 495−498.

(29) (a) Arnold, K., Bordoli, L., Kopp, J., and Schwede, T. (2006) The SWISS-MODEL Workspace: A web-based environment for protein structure homology modeling. *Bioinformatics 22*, 195−201. (b) Kiefer, F., Arnold, K., Künzli, M., Bordoli, L., and Schwede, T. (2009) The SWISS-MODEL Repository and associated resources. *Nucleic Acids Res. 37*, D387−D392. (c) Peitsch, M. C. (1995) Protein modeling by E-mail. *Bio/Technology 13*, 658−660.

(30) Hoyles, M., Kuyucak, S., and Chung, S. H. (1998) Computer simulation of ion conductance in membrane channels. *Phys. Rev. E: Stat., Nonlinear, Soft Matter Phys. 58*, 3654−3661.

(31) Mintseris, J., Pierce, B., Wiehe, K., Anderson, R., Chen, R., and Weng, Z. (2007) Integrating statistical pair potentials into protein complex prediction. *Proteins 69*, 511−520.

(32) Xu, X., and Nelson, J. W. (1993) Solution structure of tertiapin determined using nuclear magnetic resonance and distance geometry. *Proteins 17*, 124−137.

(33) Phillips, J. C., Braun, R., Wang, W., Gumbart, J., Tajkhorshid, E., Villa, E., Chipot, C., Skeel, R. D., Kale, L., and Schulten, K. (2005) Scalable molecular dynamics with NAMD. *J. Comput. Chem. 26*, 1781−1802.

(34) Humphrey, W., Dalke, A., and Schulten, K. (1996) VMD: Visual molecular dynamics. *J. Mol. Graphics 14*, 33−38.

(35) MacKerell, A. D., Jr., Feig, M., and Brooks, C. L., III (2004) Extending the treatment of backbone energetics in protein force fields: Limitations of gas-phase quantum mechanics in reproducing protein conformational distributions in molecular dynamics simulations. *J. Comput. Chem. 25*, 1400−1415.

(36) MacKerell, A. D., Jr., Bashford, D., Bellott, M., Dunbrack, R. L., Jr., Evanseck, J. D., Field, M. J., Fischer, S., Gao, J., Guo, H., Ha, S., Joseph-McCarthy, D., Kuchnir, L., Kuczera, K., Lau, F. T. K., Mattos, C., Michnick, S., Ngo, T., Nguyen, D. T., Prodhom, B., Reiher, W. E., III, Roux, B., Schlenkrich, M., Smith, J. C., Stote, R., Straub, J., Watanabe, M., Wiorkiewicz-Kuczera, J., Yin, D., and Karplus, M. (1998) All-atom empirical potential for molecular modeling and dynamic studies of proteins. *J. Phys. Chem. B 102*, 3586−3616.

(37) (a) Kumar, S., Rosenberg, J. M., Bouzida, D., Swendsen, R. H., and Kollman, P. A. (1995) Multidimensional free-energy calculations using the weighted histogram analysis method. *J. Comput. Chem. 16*, 1339−1350. (b) Grossfield, A. (2008) An implementation of WHAM: The weighted histogram analysis method. http://membrane.urmc.rochester.edu/Software/WHAM/WHAM.html (accessed August 20).

(38) Allen, T. W., Andersen, O. S., and Roux, B. (2004) Energetics of ion conduction through the gramicidin channel. *Proc. Natl. Acad. Sci. U.S.A. 101*, 117−122.

(39) Chen, R., Robinson, A., Gordon, D., and Chung, S. H. (2011) Modeling the binding of three toxins to the voltage-gated potassium channel (Kv1.3). *Biophys. J. 101*, 2652−2660.

(40) Gordon, D., Chen, R., and Chung, S. H. (2013) Computational methods of studying the binding of toxins from venomous animals to biological ions channels: Theory and application. *Physiol. Rev.*,.
(41) Jensen, M. O., Borhani, D. W., Lindorff-Larsen, K., Maragakis, P., Jogini, V., Eastwood, M. P., Dror, R. O., and Shaw, D. E. (2010) Principles of conduction and hydrophobic gating in K^+ channels. *Proc. Natl. Acad. Sci. U.S.A. 107*, 5833−5838.
(42) Corry, B. (2006) An energy-efficient gating mechanism in the acetylcholine receptor channel suggested by molecular and Brownian dynamics. *Biophys. J. 90*, 799−810.
(43) Ho, K., Nichols, C. G., Lederer, W. J., Lytton, J., Vassilev, P. M., Kanazirska, M. V., and Hebert, S. C. (1993) Cloning and expression of an inwardly rectifying ATP-regulated potassium channel. *Nature 362*, 31−38.
(44) Zhou, H., Tate, S. S., and Palmer, L. G. (1994) Primary structure and functional properties of an epithelial K channel. *Am. J. Physiol. 266*, C809−C824.
(45) Kubo, Y., Baldwin, T. J., Jan, Y. N., and Jan, L. Y. (1993) Primary structure and functional expression of a mouse inward rectifier potassium channel. *Nature 362*, 127−133.
(46) Sackin, H., Nanzashvili, M., Palmer, L. G., Krambis, M., and Walters, D. E. (2005) Structural locus of the pH gate in the Kir1.1 inward rectifier channel. *Biophys. J. 88*, 2597−2606.
(47) Jin, W., Klem, A. M., Lewis, J. H., and Lu, Z. (1999) Mechanisms of inward-rectifier K^+ channel inhibition by tertiapin-Q. *Biochemistry 38*, 14294−14301.
(48) Ramu, Y., Klem, A. M., and Lu, Z. (2001) Titration of Tertiapin-Q inhibition of ROMK1 channels by extracellular protons. *Biochemistry 40*, 3601−3605.